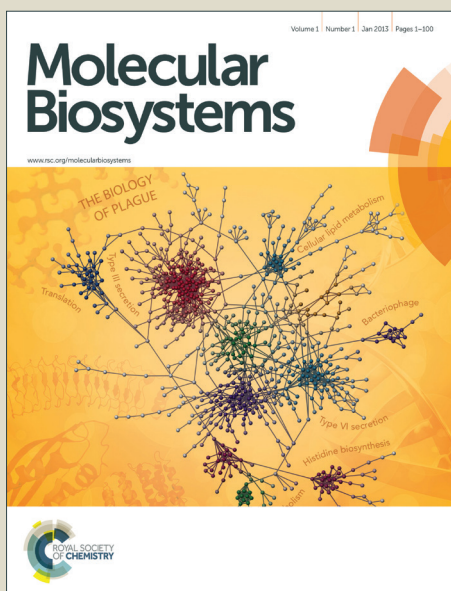


Molecular BioSystems

Accepted Manuscript



This is an *Accepted Manuscript*, which has been through the Royal Society of Chemistry peer review process and has been accepted for publication.

Accepted Manuscripts are published online shortly after acceptance, before technical editing, formatting and proof reading. Using this free service, authors can make their results available to the community, in citable form, before we publish the edited article. We will replace this *Accepted Manuscript* with the edited and formatted *Advance Article* as soon as it is available.

You can find more information about *Accepted Manuscripts* in the [Information for Authors](#).

Please note that technical editing may introduce minor changes to the text and/or graphics, which may alter content. The journal's standard [Terms & Conditions](#) and the [Ethical guidelines](#) still apply. In no event shall the Royal Society of Chemistry be held responsible for any errors or omissions in this *Accepted Manuscript* or any consequences arising from the use of any information it contains.



www.rsc.org/molecularbiosystems

Changes in the cardiac metabolome caused by perhexiline treatment in a mouse model of hypertrophic cardiomyopathy

Katja Gehmlich^{1#}, Michael S. Dodd^{2#}, J. William Allwood^{3#}, Matthew Kelly¹, Mohamed Bellahcene¹, Heena V. Lad¹, Alexander Stockenhuber¹, Charlotte Hooper¹, Houman Ashrafian¹, Charles S. Redwood^{1#}, Lucie Carrier^{4,5}, Warwick B. Dunn^{3#*}

¹ Division of Cardiovascular Medicine, Radcliffe Department of Medicine, University of Oxford, Oxford, United Kingdom

² Cardiac Metabolism Research Group, Department of Physiology, Anatomy & Genetics, University of Oxford, Oxford, United Kingdom

³ School of Biosciences, University of Birmingham, Birmingham, United Kingdom

⁴ Department of Experimental Pharmacology and Toxicology, Cardiovascular Research Centre, University Medical Center, Hamburg-Eppendorf, Hamburg, Germany

⁵ DZHK (German Centre for Cardiovascular Research), partner site Hamburg/Kiel/Lübeck, Germany

These authors contributed equally to this work.

* Corresponding Author: Dr. Katja Gehmlich

Address: Division of Cardiovascular Medicine, Radcliffe Department of Medicine, University of Oxford Level 6, West Wing, John Radcliffe Hospital, Headley Way, Headington, Oxford OX3 9DU, United Kingdom; email: katja.gehmlich@cardiov.ox.ac.uk; phone: ++44 (0)1865 234902

Abstract

Energy depletion has been highlighted as an important contributor to the pathology of hypertrophic cardiomyopathy (HCM), a common inherited cardiac disease. Pharmacological reversal of energy depletion appears an attractive approach and the use of perhexiline has been proposed as it is thought to shift myocardial metabolism from fatty acid to glucose utilisation, increasing ATP production and myocardial efficiency. We used the *Mybpc3*-targeted knock-in mouse model of HCM to investigate changes in the cardiac metabolome following perhexiline treatment. Echocardiography indicated that perhexiline induced partial improvement of some, but not all hypertrophic parameters after six weeks. Non-targeted metabolomics, applying ultra-high performance liquid chromatography-mass spectrometry, described a phenotypic modification of the cardiac metabolome with 272 unique metabolites showing a statistically significant change ($p < 0.05$). Changes in fatty acids and acyl carnitines indicate altered fatty acid transport into mitochondria, implying reduction in fatty acid beta-oxidation. Increased glucose utilisation is indirectly implied through changes in the glycolytic, glycerol, pentose phosphate, tricarboxylic acid and pantothenate pathways. Depleted reduced glutathione and increased production of NADPH suggest reduction in oxidative stress. These data delineate the metabolic changes occurring during improvement of the HCM phenotype and indicate the requirements for further targeted interventions.

Keywords

Hypertrophic cardiomyopathy; perhexiline, cardiac metabolome, UHPLC-MS, fatty acids, acyl carnitines, glycolysis, glycerol metabolism, pentose phosphate pathway, TCA cycle

1. Introduction

Hypertrophic cardiomyopathy (HCM) is a common single gene disorder of the heart characterised by left ventricular hypertrophy and myocardial disarray. HCM is associated with diastolic dysfunction and life-threatening arrhythmias, and obstruction of the left ventricular outflow tract occurs in a subset of patients. The prevalence of HCM is estimated to be 1:500¹ and it is a leading cause of sudden cardiac death in young athletes.² Molecular genetic work has shown that the majority of cases are caused by autosomal dominant mutations in genes encoding components of the contractile apparatus, in total more than 1000 mutations in over 10 genes have been identified.³ The most common disease genes are *MYH7* and *MYBPC3*, coding for β -myosin heavy chain and cardiac myosin binding protein C, respectively. Together they account for more than 80 % of cases in which a mutation has been identified.⁴

Clinically, outflow tract obstruction in human HCM can be surgically corrected by septal myectomy or by alcohol ablation.⁵ The risk of sudden cardiac death in HCM is managed by the use of implantable cardioverter defibrillators (ICD) following risk stratification.⁶ While this measure prevents sudden cardiac death in most patients,⁷ the current treatment options for diastolic dysfunction in HCM are limited and non-specific: pharmacological therapy is similar to general heart failure therapy and includes beta-blocker, verapamil, diuretics and ACE-inhibitors.⁸ Energy depletion has been highlighted as a molecular hallmark in HCM.⁹ The cardiac phosphocreatine (PCr) to adenosine triphosphate (ATP) ratio was lower in HCM patients than in controls and independent of the underlying genetic mutation.¹⁰ Mouse models and *in vitro* experiments have demonstrated cardiac myocyte energy depletion due to inefficient ATP utilization and altered intracellular calcium handling (for review, see¹¹). Consequently, pharmacological metabolic modulation reversing this energy depletion appears an attractive concept for the treatment of HCM.

Perhexiline (2-(2,2-dicyclohexylethyl)piperidine) maleate (referred to as perhexiline in this manuscript) is a potent inhibitor of the carnitine palmitoyltransferase-1 (CPT1) and to a lesser extent of carnitine palmitoyltransferase-2 (CPT2).¹² The inhibition of these enzymes blocks the import of long-chain fatty acids (C₁₄-C₂₀) into the mitochondria for beta-oxidation and is thereby thought to shift myocardial metabolism from fatty acid to glucose utilisation.¹³ As a consequence ATP production is increased at the same oxygen consumption, and hence myocardial efficiency is improved.¹⁴ In parallel, vasodilation of coronary arteries is also observed following treatment with perhexiline.¹⁵ The drug is in use as an anti-anginal drug in Australia and New Zealand,¹⁶ but its narrow therapeutic index and potential toxicity in poor metabolisers have prevented a wider application as anti-anginal drug, as alternative drugs with excellent proven efficacy are available. However, perhexiline belongs to the drugs which are revisited as specific therapeutic agents for a much smaller group of patients, namely individuals suffering from HCM. It was recently shown that perhexiline can improve myocardial energetics, i.e. increase PCr to ATP ratios in HCM patients.¹⁷ More importantly, in this randomized, double-blind, placebo-controlled, parallel-group study on 46 HCM patients, it was shown that perhexiline treatment improved exercise capacity and symptomatic outcome. Thus perhexiline appears an attractive candidate drug for the treatment of HCM. However, the exact mechanisms underlying its clinical benefit are still unclear: in addition to CPT1/CPT2 inhibition, NADP oxidase

inhibition and nitric oxide potentiation are discussed as potential modes of action.¹⁸ To gain more detailed insight into the molecular actions of perhexiline, wild-type (WT) mice were treated with the drug and subjected to proteomic and metabolomic analyses.¹⁹ This previous study found that perhexiline altered metabolic substrate use from free fatty acid to lactate through enzymatic changes in glucose and lipid metabolism including acyl-CoA dehydrogenases and decreased phosphorylation of the pyruvate dehydrogenase complex. Other metabolic changes included decreased levels of acetate, taurine and creatine and computational modelling of the data implicated changes in tricarboxylic acid (TCA) cycle metabolism and substrate use.

A *Mybpc3*-targeted knock-in (*Mybpc3* KI) mouse model has been generated to mimic a human *MYBPC3* HCM mutation.²⁰ Homozygous mice display pronounced cardiac hypertrophy and diastolic dysfunction,²¹ thereby mimicking the main characteristics of human HCM. These *Mybpc3* KI mice provide a powerful tool for invasive investigations of HCM,²¹⁻²³ including testing novel potential therapeutic options. To investigate in significant depth the metabolic consequences of perhexiline treatment, we treated *Mybpc3* KI mice with either perhexiline or a placebo for 6 weeks and investigated changes in the metabolic profile of cardiac tissue applying ultra-high performance liquid chromatography-mass spectrometry (UHPLC-MS).

2. Materials and Methods

2.1 Ethical statement

Experimental procedures were performed in accordance with the UK Home office guidelines (project licenses 30/2444 and 30/2977) and approved by respective institutional review boards.

2.2 Animal husbandry and perhexiline treatment

Homozygous male *Mybpc3* KI mice,²⁰ which were backcrossed onto the C57BL/6J background in Hamburg, and age-matched C57BL/6J WT mice (Harlan) were maintained in individually ventilated cages on a 12 hr light/dark cycle with food and water *ad libitum*. *Mybpc3* KI mice were subjected to perhexiline treatment (n = 6) or placebo treatment (n = 6). Non-treated WT animals (n = 8) were used as controls in left ventricular haemodynamic measurements and for *ex vivo* phenotyping.

Perhexiline (2-(2,2-Dicyclohexylethyl)piperidine maleate) was purified from crushed PEXSIG tablets (Sigma Pharmaceuticals Ltd, Australia) by re-crystallisation with warm methanol. After air drying, the perhexiline was dissolved in 1.8 % (w/v) Hydroxyl-propyl-beta-cyclodextrin (Sigma) in saline and filter sterilised (final concentration 1 mg/ml), aliquots were stored at -20 °C for up to one week. Perhexiline of 100% purity was not commercially available and therefore this method for preparation was required. Perhexiline was recrystallized in methanol because it is not fully soluble in water and the excipients in the tablets (especially purified talc) are insoluble in aqueous solutions.

Eight-week-old *Mybpc3* KI animals were treated for 6 weeks with perhexiline at a dose of 30 mg/kg of body weight (BW) per day, given in two equal doses via intraperitoneal (IP) injection. Litter mates were placebo treated by injecting the same volume of sterile 1.8 % (w/v) Hydroxyl-propyl-beta-cyclodextrin (Sigma) in saline twice a day. Body weight was monitored twice weekly and injection volumes adjusted accordingly. No differences in body weight were observed between the groups (Figure 1).

2.3 Mouse phenotyping

2.3.1 Mouse echocardiography

After the 6-week-treatment period, mice were lightly anaesthetised using 1-1.5% isoflurane and imaged with a 22 to 55MHz linear array transducer using the Vevo 2100 ultrasound system (Visualsonics). M-mode tracings of short-axis images were obtained via the left parasternal window and used to measure the left ventricular end-diastolic (LVEDD) and end-systolic (LVESD) chamber dimensions and the anterior and posterior wall thickness based on measurements averaged from at least 3 separate cardiac cycles. Heart rate was recorded throughout. Left ventricular fractional shortening (FS) was calculated with the formula: $FS = (LVEDD - LVESD) / LVEDD$. Left ventricular mass (LV mass, corrected) was calculated using following formula: $LV\ mass\ (corrected) = 0.8 * 1.053 * ((LVID;d + LVPW;d + IVS;d)^3 - LVID;d^3)$, whereby LVID;d is end-diastolic left ventricular internal dimension, LVPW;d end-diastolic left ventricular posterior wall thickness and IVS;d is end-diastolic intraventricular septum width.

2.3.2 Left ventricular haemodynamics

The mice were anaesthetised with isoflurane (1.25–1.5%) for the measurement of haemodynamic indices using a 1.4 F Millar Mikro-tip catheter (SPR-671) inserted into the LV via the carotid artery. After 15 min of baseline recordings, contractile reserve was assessed by infusion of dobutamine via the jugular vein (4-16 ng/g bodyweight/min).²⁴

2.3.3 Plasma and cardiac tissue collection

After the procedure, blood was collected by cardiac puncture and EDTA plasma samples (microvette CB 300, Sarstedt) were snap frozen in liquid nitrogen and stored at -80 °C until measurement of achieved perhexiline levels by high-performance liquid chromatography (HPLC) (Cardiff Toxicology Laboratories, University Hospital Llandough). Whole hearts were excised, weighed, rinsed in saline and snap frozen in liquid nitrogen. The time from excision to snap freezing was less than one minute. Tibia length was determined after digestion in 0.8 M potassium hydroxide overnight.

2.3.4 Reverse transcriptase–quantitative polymerase chain reaction (RT-qPCR)

Total RNA was extracted from snap-frozen and pulverized heart tissue using the RNeasy Fibrous Tissue Mini Kit (Qiagen). For RT-qPCR 1 µg of total RNA was reverse transcribed with High Capacity cDNA Reverse transcription Kit (Applied Biosystems) prior to amplification reactions performed using Fast Universal Master Mix on a StepOnePlus system (Applied Biosystems). Samples were run in duplicates in a total reaction volume of 10 µl. Following inventoried Taqman assays (Applied Biosystems) were used: atrial natriuretic peptide (*Nppa* Mm01255748_g1), brain natriuretic peptide (*Nppb* Mm01255770_g1), alpha-skeletal actin (*Acta1* Mm00808218_g1), collagen, type I, alpha 1 (*Col1a* Mm00801666_g1), collagen, type 3, alpha (*Col3a*, Mm01254476_m1), matrix metalloproteinase 2 (*Mmp2*, Mm00439498_m1), matrix metalloproteinase 9 (*Mmp9*, Mm00442991_m1). The relative quantities of target gene mRNA levels were normalised against the endogenous control Glyceraldehyde 3-phosphate dehydrogenase (*Gapdh*, 4352932E, Applied Biosystems) and relative expression was quantified using the comparative CT method. Four hearts from age-matched C57BL/6J male mice served as WT control group.

2.3.5 Evaluation of fibrosis at protein level

Western blotting was performed as described previously,²² using the following antibodies: anti-collagen 1 (Novus biologicals, polyclonal rabbit, NB600-408) and anti-calsequestrin (Thermo Scientific, polyclonal rabbit, PA1-913) as loading control. For hydroxyproline measurement, aliquots (n=5 per group) of the powdered heart tissue were hydrolysed in 6M HCl at 95°C for 20 hours. The amount of collagen in these samples was determined by measuring hydroxyproline content by colorimetric assay (Quickzyme Biosciences, as per manufacturer's instructions), modifying the hydroxyproline residues using chloramineT/DMBA, resulting in a coloured product at 570 nm OD.

2.3.6 Statistics

Values are given as mean +/- standard error of mean. A one-way ANOVA test followed by Bonferroni post-hoc test was used to compare differences among multiple groups. To compare two unpaired sample groups, Student's t-test was performed. $p < 0.05$ was assumed to be significant.

2.4 Metabolic profiling study

2.4.1 Sampling and extraction of cardiac tissue

All solvents and chemicals applied were of HPLC analytical grade (J.T. Baker, U.K.). 6 samples from placebo-treated and 6 samples from perhexiline-treated animals were studied. Mouse cardiac tissues from different animals were weighed (range=108-168 mg) and subsequently extracted in a randomised order in Precellys ceramic bead soft tissue homogenisation tubes (Bertin Technologies, Stretton Scientific U.K.). An extraction solution of 2.5:1:1 of methanol:chloroform:water cooled to -20 °C was applied to perform a monophasic extraction with the volume applied normalised to tissue weight (9.2 µL per mg tissue). Homogenisation was performed in a Precellys 24 homogeniser (Bertin

Technologies, Stretton Scientific U.K.) with the following homogenisation cycle; 6400 rpm for 15 sec, 0 rpm for 15 sec and 6400 rpm for 15 sec. The tubes were then centrifuged at 3 °C and 10,000g for 5 min to pellet the cardiac tissue. 450 µL were transferred to 2.0 mL microcentrifuge tubes and dried under a nitrogen gas stream prior (room temperature) prior to storage at -80 °C until analysis. An additional homogenisation tube, without cardiac tissue, was employed to generate a blank control sample. Quality control (QC) samples,²⁵⁻²⁶ were prepared by pooling all remaining extraction supernatants followed by transfer of 450µL aliquots to 2.0 mL microcentrifuge tubes followed by drying under a nitrogen gas stream (room temperature) prior to storage at -80 °C until analysis.

2.4.2 Metabolic profiling of cardiac tissue

All solvents and chemicals applied were of HPLC analytical grade (J.T. Baker, U.K.). UHPLC-MS analysis of tissue extracts and QC samples was performed applying a Dionex U3000 coupled to an electrospray LTQ-FT-MS Ultra mass spectrometer (Thermo Scientific Ltd. UK). Samples were reconstituted in 50 µL of 50:50 methanol:water, vortex mixed and centrifuged for 15 min at 10,000 g and transferred to vials with 200 µL fixed inserts (Thermo-Fisher Ltd. U.K.). All samples were stored in the autosampler at 5 °C and analysed separately in negative and positive electrospray ionisation (ESI) modes within 72 h of reconstitution. UHPLC separations were performed applying a Hypersil Gold C₁₈ reversed phase column (100 x 2.1mm, 1.9µm) at a flow rate of 400 µL/min, temperature of 40 °C and with two solvents: solvent A (HPLC grade water + 0.1% formic acid) and solvent B (HPLC grade methanol + 0.1% formic acid). A gradient elution was performed as follows: hold 100% A 0-1.5 min, 100% A - 100% B 1.5-6 min curve 3, hold 100% B 6-12 min, 100% B – 100% A 12-13 min curve 3, hold 100% A 13-15 min. Injection volume was 5µL. UHPLC eluent was introduced directly in to the electrospray LTQ-FT Ultra mass spectrometer with source conditions as follows: spray voltage -4.5 kV (ESI-) and +5 kV (ESI+), sheath gas 30 arbitrary units, aux gas 15 arbitrary units, capillary voltage 35 V, tube lens voltage -100 V (ESI-) and +90 V (ESI+), capillary temperature 280 °C, ESI heater temperature 300 °C. Data were acquired in the FT mass spectrometer in the *m/z* range 100-1000 at a mass resolution of 50,000 (FWHM defined at *m/z* 400), with a scan speed of 0.4 sec and an AGC setting of 1x10⁶. Analysis order was composed of 10 QC sample injections for system conditioning followed by a QC sample injection every 6th injection with two QC sample injections at the end of the analytical run. Tissue extracts were analysed in a random order.

UHPLC-MS raw data profiles were first converted into a NetCDF format within the Xcalibur software's File Converter program. Each NetCDF based three-dimensional data matrix (intensity x *m/z* x time – one per sample) was converted (or deconvolved) into a vector of peak responses, where a peak response is defined as the sum of intensities over a window of specified mass and time range (e.g. *m/z* = 102.1 ± 0.01 and time = 130 ± 10 s). In this experiment the deconvolution was performed using the freely available XCMS software as described previously and in Supplementary Table SI-4.²³ Data were exported from XCMS as a .csv file for further data analysis. The quality of data was assessed applying QC data as previously described,²⁵ with all metabolite features with a RSD>20% for QC samples being removed from the dataset prior to data analysis. The data for each sample was normalised (as a percentage) to the total peak area for all metabolites in the sample. Metabolite

annotation was performed applying the PUTMEDID_LCMS workflow as previously described.²⁷ All metabolite annotations are reported at level 2 (putatively annotated compounds) according to MSI reporting standards.²⁸ In cases where a single metabolite is detected as multiple metabolite features (as described previously²⁹), only a single feature is reported chosen as having a critical p-value nearest to 0.05. The processed data was analysed in R applying the unsupervised multivariate principal components analysis (PCA) and the univariate non-parametric Wilcoxon–Mann–Whitney test. No correction for false discovery rate was applied. The fold change (median perhexiline-treated/median placebo-treated) was calculated including 95% confidence limits. Metabolites were manually clustered in to classes defining similar chemical structure or metabolic pathway to identify biologically relevant and robust metabolic changes.

3. Results

The influence of perhexiline on cardiac metabolism was investigated in a *Mybpc3* KI mouse model,²⁰ which mimics a human HCM mutation in *MYBPC3*, the most common HCM disease gene. Six mice were treated with perhexiline (30 mg/kg body weight per day by IP injection) for 6 weeks and compared to placebo-treated littermates. After this period cardiac parameters of the mice were assessed and cardiac tissue was collected and subjected to non-targeted metabolic profiling. Hydrophilic and lipophilic metabolites were extracted using a monophasic solution and analysed using UHPLC-MS; in total 25 biological and QC samples were examined.

3.1. Perhexiline and hydroxyl-perhexiline changes in cardiac tissue

The average perhexiline concentration in the plasma of treated animals was 0.59 +/- 0.16 mg/L, the average concentration of its primary metabolite hydroxy-perhexiline was 0.07 +/- 0.08 mg/L. Both the achieved perhexiline concentration and the hydroxy-perhexiline to perhexiline ratio are within the recommended range for human therapeutic application (perhexiline concentration 0.15 – 0.60 mg/L, hydroxy-perhexiline to perhexiline ratio <= 0.3).³⁰ The concentration of perhexiline in cardiac tissue was not quantified, though its presence in perhexiline-treated animals and absence in placebo-treated animals was observed in the non-targeted metabolomics study (Figure SI-1).

3.2. Phenotypic changes

Upon completion of perhexiline treatment, echocardiographic parameters indicative of cardiac hypertrophy were altered: the LV anterior wall thickness was found to be reduced in perhexiline-treated mice, as well as the calculated LV mass (Figure 1). However, no changes in global morphometric parameters of cardiac hypertrophy (such as heart weight to body weight or heart weight to tibia length ratio) were observed (Table SI-1). Moreover, left ventricular haemodynamic function did not change significantly in *Mybpc3* KI mice upon perhexiline treatment (Table SI-2), in agreement with unaltered LV fractional shortening on echocardiography (Figure 1). Taken together, these data indicate that perhexiline may induce a partial improvement of the hypertrophic phenotype in the

mouse model, which can be assessed by sensitive echocardiography; however the treatment did not completely reverse the pronounced HCM phenotype of the mouse model. In agreement with these findings, mRNA levels of markers of cardiac hypertrophy (*Nppa*, *Nppb*, *Acta1*) were higher in the *Mybpc3* KI than in WT mice, but no major differences were observed between perhexiline- and placebo-treated *Mybpc3* KI mice (Figure SI-2). Of note, perhexiline-treatment led to a reduced type 1 collagen mRNA level (Figure SI-3), a marker for fibrosis, again implying partial regression of the HCM phenotype. For other markers of fibrosis (collagen 3, matrix metalloproteinases 2 and 9)²⁴ a similar visual trend was observed, but not reaching statistical significance (Figure SI-3). However, collagen 1 protein levels were not altered between perhexiline-treated and placebo-treated animals (Figure SI-4).

3.3. Non-targeted UHPLC-MS metabolomics

Non-targeted metabolomics applying UHPLC-MS provided the detection of 6364 and 6362 metabolite features in positive and negative ion modes, respectively. The reproducibility of data was very good as expected for a small analytical batch length. Those metabolites with a RSD>20% as determined in QC samples were removed from the dataset before further data analysis was performed. In negative ion mode 4055 of 6360 metabolites features remained and in positive ion mode 5117 of 6362 metabolite features remained after quality control. Unsupervised multivariate PCA was performed to assess the biological and technical variation of the data. No visual separation of perhexiline-treated and placebo-treated animals was observed in PCs 1 to 3 in negative ion mode. Some separation of perhexiline-treated and placebo-treated animals was observed in PC1 vs. PC3 for positive ion mode data. These results highlight a potential (but not conclusive) metabolic perturbation being present in relation to perhexiline treatment (Figure 2); future work is planned to validate these discoveries. The PCA loadings plot showed no clear indication of the metabolites providing the greatest separation power to the PCA scores plot. To assess the metabolic disturbance further we performed univariate analysis to define metabolites which showed a statistically significant difference ($p<0.05$) between the two classes. As false discovery is present in these studies we then grouped metabolites based on metabolic function or structural similarity, the probability of multiple and related metabolites being observed as statistically significant and being false discoveries decreases as the number of metabolites in each class increases. The groups of metabolites showing a robust biological difference between classes and discussed below are shown in Table 1 with all data available in supplementary information (Table SI-3). In total 272 unique metabolite(s) were observed to be statistically significant ($p<0.05$) and these were grouped in to 13 classes. The potential biological mechanisms associated with these reported metabolic changes are presented in the Discussion section below.

4. Discussion

Perhexiline inhibits the action of CPT1 and CPT2.¹⁸ The inhibition of these enzymes blocks the import of long-chain fatty acids into the mitochondria for beta-oxidation and therefore is proposed to

shift myocardial metabolism from fatty acid to glucose utilisation. Here we studied the effect of perhexiline treatment on the cardiac metabolome in *Mybpc3* KI mice, with plasma perhexiline concentrations similar to those attained during treatment of HCM in humans.¹⁷ We applied a non-targeted metabolomics approach using a monophasic extraction method and a reversed phase UHPLC-MS approach to construct a metabolic profile for each sample composed of both hydrophilic and lipophilic metabolites. PCA showed a separation of perhexiline-treated and placebo-animals in positive ion mode UHPLC-MS only (PC1 vs. PC3) and this was studied further applying univariate analysis. The major findings of the study are metabolic disturbances related to fatty acid and glucose metabolism as well as a potential change in oxidative stress and these will be discussed in further detail.

4.1. Changes in long chain fatty acids and acyl carnitines

Long chain fatty acids, including octadecadienoic acid and icosatetraenoic acid/eicosatetraenoic acid showed a decrease in the cardiac metabolome of perhexiline-treated animals; this is consistent with the predicted inhibition of CPT1 and CPT2 resulting in a reduction in the transport of fatty acids into cardiac mitochondria. There were perturbations in the concentration of eight acyl carnitines following perhexiline treatment, though both increases (e.g. butanoyl and decanoyl carnitine) and decreases (e.g. octanoyl and acetyl carnitine) were observed (Table 1). Interestingly, taurine and creatinine were elevated in perhexiline-treated animals (Table 1) in agreement with a previous report that showed similar variation of taurine and creatine (the precursor of creatinine).¹⁹ This validates both the approach we have applied and the previous findings. However, other biologically interesting changes were observed: alterations indicative to changes in oxidative stress, changes in glycerol pathways, in TCA metabolites and in tryptophan/tyrosine metabolic pathways.

4.2. Oxidative stress

First, oxidative stress has been implicated in HCM and increased ratios of oxidised to reduced glutathione indicate higher levels of oxidative stress.³¹⁻³² In our study perhexiline treatment increased the level of reduced glutathione (Table 1) implying that treatment reduces oxidative stress in tissues, a positive outcome (although there has been no study, and therefore confirmation, of oxidative stress in *Mybpc3* KI mice). Oxidised glutathione was not detected in our study. NADPH is used to regenerate reduced glutathione with the major source of NADPH production deriving from the oxidative phase of the pentose phosphate pathway. In this study an increase in the concentration of ribulose-5-phosphate/ribose-5-phosphate, the products of the oxidative phase of the pentose phosphate pathway, support an increased synthesis of NADPH and suggests that a greater level of glutathione regeneration by NADPH in perhexiline-treated animals is present. Although speculative, this increase may be a result of an increased flux through glycolysis, as discussed below, and therefore a higher availability of substrates for the pentose phosphate pathway.

4.3. Glycerol metabolism

Second, changes in glycerol metabolism have been observed in this study. The concentrations of glycerol and glycerol-3-phosphate are reduced following perhexiline treatment (Table 1). This could have several implications in the heart. These lower concentrations could be due to an increase in storage of excess fatty acids as triacylglycerols, though no triacylglycerols were detected in this study. Additionally choline and glycerophosphocholine increased following perhexiline treatment indicating a potential decrease in glycerophospholipid synthesis; however no decrease in glycerophospholipids was observed in this study, even though these metabolites were detected. Alternatively the decrease in glycerol and glycerol-3-phosphate could be due to increased activity of glycerol-3-phosphate dehydrogenase (G3PDH). This enzyme is responsible for the generation of dihydroxyacetone phosphate (DHAP), for use in glycolysis and the mitochondrial G3PDH is also coupled to complex II of the electron transport chain (ETC), therefore generating ATP directly through the ETC and indirectly through supplementation of glycolysis. This latter hypothesis is strengthened by a reduction in DHAP and glyceraldehyde-3-phosphate (GAP) levels in the perhexiline treated animals, indicating increased use of these glycolytic intermediates. These changes potentially indicate that the expected increased use of glucose is being mediated through changes both in glycolysis as discussed here and in the pentose phosphate pathway as discussed above.

4.4. TCA cycle

Third, we also observed changes in the concentration of four TCA metabolites. Citrate/isocitrate showed an increase in concentration and this may imply an increased entry of acetyl-CoA into the TCA cycle where the first two metabolites are citrate and isocitrate. This observed change may indicate increased production of acetyl-CoA through glycolysis, supporting the hypothesis of increased flux through glycolysis, though this could also be a result of an increase in fatty acid beta-oxidation. Although we cannot differentiate between mechanisms without further studies, as a reduction in fatty acid beta-oxidation is implied from changes in fatty acids and acyl carnitines, we can hypothesise that an increased flux of acetyl-CoA into the TCA cycle is a result of increased glycolytic flux. Of interest is that five related metabolites in pantothenate metabolism and involved in CoA synthesis all showed changes in perhexiline treated animals. Pantothenate, pantoate, 4-phosphopantothenate and pantetheine-4-phosphate all increased following treatment whereas pantetheine concentration decreased, suggesting that increased synthesis of CoA with predicted impact on acetyl-CoA production, consistent with the observed increase in citrate/isocitrate. In the TCA cycle, malate also showed an increased concentration in perhexiline treated animals. Two metabolically-linked metabolites, fumarate and succinate showed a decreased concentration in perhexiline-treated animals which may relate to a change in oxidative phosphorylation as both are involved in complex II of the ETC.

4.5. Aromatic amino acids

Finally, the aromatic amino acids tryptophan and tyrosine and associated metabolites showed changes in perhexiline-treated animals. Tryptophan and tyrosine showed an increase in perhexiline-treated animals whereas 5-hydroxytryptophan, hydroxykynurenine and tryptamine, all metabolic

derivatives of tryptophan, showed a decrease in treated animals. Understanding serotonin (5-hydroxytryptamine, a related derivative of tryptophan) regulation of cardiovascular function has been reviewed recently³³ and maternal serotonin level has been shown to inversely correlate to severity of the cardiac phenotype in the offspring of HCM animals.³⁴ Papers in the 1970s reported that tryptophan prophylaxis in African patients liable to cardiomyopathy led to reduced serotonin levels³⁵ and serotonin levels in the failing myopathic hamster heart are reduced compared to healthy controls.³⁶

5. Conclusions

The present work applied non-targeted metabolomics to identify changes in the cardiac metabolome of a HCM animal model (*Mybpc3* KI mouse model) related to a partial improvement of the hypertrophic phenotype following perhexiline treatment for six weeks. Changes in fatty acid and acyl carnitine levels were observed linked to the inhibition of CPT1 and CPT2, the target of perhexiline. However, the metabolic perturbation observed was complex and a number of changes cannot be directly related to these known targets of perhexiline. Changes in the cardiac metabolome related to glycolysis, glycerol metabolism, the pentose phosphate pathway, TCA cycle, pantothenate metabolism and aromatic amino acid metabolism were also observed. The results provide evidence of a diverse, but potentially linked, set of metabolic changes related to perhexiline treatment and an improved hypertrophic phenotype. The study has also shown the sensitivity of applying metabolomics to define and investigate phenotypic changes compared to non-molecular techniques. The study has enabled us to construct hypotheses for further testing in targeted biological studies focused on (i) the interaction of glycolysis, pentose phosphate pathway, pantothenate and TCA metabolism and (ii) fatty acid and acyl carnitine metabolism.

There were some limitations to the study. Perhexiline treatment did not reverse the pronounced HCM phenotype in *Mybpc3* KI mice, only individual echo parameters (Figure 1) and type 1 collagen mRNA (Figure SI-3), but not protein (Figure SI-4), showed partial improvement. Longer treatment or a higher dose of the drug might be required to normalise the HCM phenotype substantially. No post-mortem LV weight/dimension data are available to validate the echocardiographic findings. WT mice were not subjected to the same treatment regime, hence no data on WT control mice are available for cardiac function under this drug treatment, or for metabolomics. The metabolic profiling study applied a small number of animals in each class (n=6) and further studies will apply larger sample numbers and a targeted approach to validate changes observed in the metabolic pathways identified above.

Supporting Information

Figure SI-1. Extracted Ion Chromatograms representing perhexiline in placebo-treated and perhexiline-treated mice. Figure SI-2. Molecular parameters of hypertrophy in perhexiline- and placebo-treated *Mybpc3* KI mice compared to WT mice. Figure SI-3. Molecular parameters of fibrosis

in perhexiline- and placebo-treated *Mybpc3* KI mice compared to WT mice. Figure SI-4. Collagen 1 protein levels in perhexiline- and placebo-treated *Mybpc3* KI mice.

Table SI-1. Morphometric data on perhexiline- and placebo-treated *Mybpc3* KI mice compared to WT mice. Table SI-2. Left ventricular haemodynamic measurements on perhexiline- and placebo-treated *Mybpc3* KI mice compared to WT. Table SI-3. List of statistically significant metabolites when comparing placebo-treated vs. perhexiline-treated mice. Table SI-4. XCMS parameters.

Author Contributions

KG - study initiation, experimental planning, logistics and coordination, animal experiments and phenotyping and manuscript preparation; MD, JWA, WBD – metabolomics study and metabolic data interpretation and manuscript preparation; MK, MB, HL, – animal experiments and phenotyping and manuscript preparation; LC – provision of animals and manuscript revision; CH, AS – ex-vivo analysis and manuscript preparation; KG, HA, CR – study initiation, experimental planning, logistics and coordination, manuscript preparation.

Conflicts of Interest

The authors declare no competing financial or other conflicts of interest.

Acknowledgements

The work was supported by the European Commission Framework Seven Grant “BIG-Heart” (241577), the British Heart Foundation Centre of Excellence at Oxford and the Wellcome Trust. JWA and WBD are supported by the Systems Science for Health Initiative at The University of Birmingham. The FT-ICR mass spectrometer used in this research was obtained through the Birmingham Science City Translational Medicine:Experimental Medicine Network of Excellence project, with support from Advantage West Midlands (AWM).

References

1. Maron, B. J., Hypertrophic cardiomyopathy: a systematic review. *JAMA : the journal of the American Medical Association* **2002**, *287* (10), 1308-20.
2. Ostman-Smith, I.; Rossano, J. W.; Shaddy, R. E., Hypertrophic cardiomyopathy: do sudden death prevention strategies in children differ between Europe and North America? *Current opinion in cardiology* **2013**, *28* (2), 130-8.
3. Watkins, H.; Ashrafian, H.; Redwood, C., Inherited cardiomyopathies. *The New England journal of medicine* **2011**, *364* (17), 1643-56.
4. Richard, P.; Charron, P.; Carrier, L.; Ledeuil, C.; Cheav, T.; Pichereau, C.; Benaiche, A.; Isnard, R.; Dubourg, O.; Burban, M.; Gueffet, J. P.; Millaire, A.; Desnos, M.; Schwartz, K.; Hainque, B.; Komajda, M.; Project, E. H. F., Hypertrophic cardiomyopathy: distribution of disease genes, spectrum of mutations, and implications for a molecular diagnosis strategy. *Circulation* **2003**, *107* (17), 2227-32.
5. Maron, B. J., Commentary and re-appraisal: surgical septal myectomy vs. alcohol ablation: after a decade of controversy and mismatch between clinical practice and guidelines. *Progress in cardiovascular diseases* **2012**, *54* (6), 523-8.
6. Maron, B. J., Risk stratification and role of implantable defibrillators for prevention of sudden death in patients with hypertrophic cardiomyopathy. *Circulation journal : official journal of the Japanese Circulation Society* **2010**, *74* (11), 2271-82.
7. Elliott, P.; Spirito, P., Prevention of hypertrophic cardiomyopathy-related deaths: theory and practice. *Heart* **2008**, *94* (10), 1269-75.
8. Semsarian, C.; Group, C. C. G. D. C. W., Guidelines for the diagnosis and management of hypertrophic cardiomyopathy. *Heart, lung & circulation* **2011**, *20* (11), 688-90.
9. Ashrafian, H.; Redwood, C.; Blair, E.; Watkins, H., Hypertrophic cardiomyopathy: a paradigm for myocardial energy depletion. *Trends in genetics : TIG* **2003**, *19* (5), 263-8.
10. Crilley, J. G.; Boehm, E. A.; Blair, E.; Rajagopalan, B.; Blamire, A. M.; Styles, P.; McKenna, W. J.; Ostman-Smith, I.; Clarke, K.; Watkins, H., Hypertrophic cardiomyopathy due to sarcomeric gene mutations is characterized by impaired energy metabolism irrespective of the degree of hypertrophy. *Journal of the American College of Cardiology* **2003**, *41* (10), 1776-82.
11. Ferrantini, C.; Belus, A.; Piroddi, N.; Scellini, B.; Tesi, C.; Poggesi, C., Mechanical and energetic consequences of HCM-causing mutations. *Journal of cardiovascular translational research* **2009**, *2* (4), 441-51.
12. Kennedy, J. A.; Unger, S. A.; Horowitz, J. D., Inhibition of carnitine palmitoyltransferase-1 in rat heart and liver by perhexiline and amiodarone. *Biochemical pharmacology* **1996**, *52* (2), 273-80.

13. Jeffrey, F. M.; Alvarez, L.; Diczku, V.; Sherry, A. D.; Malloy, C. R., Direct evidence that perhexiline modifies myocardial substrate utilization from fatty acids to lactate. *Journal of cardiovascular pharmacology* **1995**, *25* (3), 469-72.
14. Ashrafian, H.; Horowitz, J. D.; Frenneaux, M. P., Perhexiline. *Cardiovascular drug reviews* **2007**, *25* (1), 76-97.
15. Kennedy, J. A.; Mohan, P.; Pelle, M. A.; Wade, S. R.; Horowitz, J. D., The effects of perhexiline on the rat coronary vasculature. *European journal of pharmacology* **1999**, *370* (3), 263-70.
16. Horowitz, J. D.; Button, I. K.; Wing, L., Is perhexiline essential for the optimal management of angina pectoris? *Australian and New Zealand journal of medicine* **1995**, *25* (2), 111-3.
17. Abozguia, K.; Elliott, P.; McKenna, W.; Phan, T. T.; Nallur-Shivu, G.; Ahmed, I.; Maher, A. R.; Kaur, K.; Taylor, J.; Henning, A.; Ashrafian, H.; Watkins, H.; Frenneaux, M., Metabolic modulator perhexiline corrects energy deficiency and improves exercise capacity in symptomatic hypertrophic cardiomyopathy. *Circulation* **2010**, *122* (16), 1562-9.
18. Horowitz, J. D.; Chirkov, Y. Y., Perhexiline and hypertrophic cardiomyopathy: a new horizon for metabolic modulation. *Circulation* **2010**, *122* (16), 1547-9.
19. Yin, X.; Dwyer, J.; Langley, S. R.; Mayr, U.; Xing, Q.; Drozdov, I.; Nabeebaccus, A.; Shah, A. M.; Madhu, B.; Griffiths, J.; Edwards, L. M.; Mayr, M., Effects of perhexiline-induced fuel switch on the cardiac proteome and metabolome. *Journal of molecular and cellular cardiology* **2013**, *55*, 27-30.
20. Vignier, N.; Schlossarek, S.; Fraysse, B.; Mearini, G.; Kramer, E.; Pointu, H.; Mougnot, N.; Guiard, J.; Reimer, R.; Hohenberg, H.; Schwartz, K.; Vernet, M.; Eschenhagen, T.; Carrier, L., Nonsense-mediated mRNA decay and ubiquitin-proteasome system regulate cardiac myosin-binding protein C mutant levels in cardiomyopathic mice. *Circulation research* **2009**, *105* (3), 239-48.
21. Fraysse, B.; Weinberger, F.; Bardswell, S. C.; Cuello, F.; Vignier, N.; Geertz, B.; Starbatty, J.; Kramer, E.; Coirault, C.; Eschenhagen, T.; Kentish, J. C.; Avkiran, M.; Carrier, L., Increased myofilament Ca²⁺ sensitivity and diastolic dysfunction as early consequences of Mybpc3 mutation in heterozygous knock-in mice. *Journal of molecular and cellular cardiology* **2012**, *52* (6), 1299-307.
22. Gedicke-Hornung, C.; Behrens-Gawlik, V.; Reischmann, S.; Geertz, B.; Stimpel, D.; Weinberger, F.; Schlossarek, S.; Precigout, G.; Braren, I.; Eschenhagen, T.; Mearini, G.; Lorain, S.; Voit, T.; Dreyfus, P. A.; Garcia, L.; Carrier, L., Rescue of cardiomyopathy through U7snRNA-mediated exon skipping in Mybpc3-targeted knock-in mice. *EMBO molecular medicine* **2013**, *5* (7), 1060-77;
23. Schlossarek, S.; Englmann, D. R.; Sultan, K. R.; Sauer, M.; Eschenhagen, T.; Carrier, L., Defective proteolytic systems in Mybpc3-targeted mice with cardiac hypertrophy. *Basic research in cardiology* **2012**, *107* (1), 235.
24. Ten Hove, M.; Chan, S.; Lygate, C.; Monfared, M.; Boehm, E.; Hulbert, K.; Watkins, H.; Clarke, K.; Neubauer, S., Mechanisms of creatine depletion in chronically failing rat heart. *Journal of molecular and cellular cardiology* **2005**, *38* (2), 309-13.

25. Dunn, W. B.; Broadhurst, D.; Begley, P.; Zelena, E.; Francis-McIntyre, S.; Anderson, N.; Brown, M.; Knowles, J. D.; Halsall, A.; Haselden, J. N.; Nicholls, A. W.; Wilson, I. D.; Kell, D. B.; Goodacre, R.; Human Serum Metabolome, C., Procedures for large-scale metabolic profiling of serum and plasma using gas chromatography and liquid chromatography coupled to mass spectrometry. *Nature protocols* **2011**, *6* (7), 1060-83;
26. Dunn, W. B.; Wilson, I. D.; Nicholls, A. W.; Broadhurst, D., The importance of experimental design and QC samples in large-scale and MS-driven untargeted metabolomic studies of humans. *Bioanalysis* **2012**, *4* (18), 2249-64.
27. Brown, M.; Wedge, D. C.; Goodacre, R.; Kell, D. B.; Baker, P. N.; Kenny, L. C.; Mamas, M. A.; Neyses, L.; Dunn, W. B., Automated workflows for accurate mass-based putative metabolite identification in LC/MS-derived metabolomic datasets. *Bioinformatics* **2011**, *27* (8), 1108-12.
28. Sumner, L. W.; Amberg, A.; Barrett, D.; Beale, M. H.; Beger, R.; Daykin, C. A.; Fan, T. W.; Fiehn, O.; Goodacre, R.; Griffin, J. L.; Hankemeier, T.; Hardy, N.; Harnly, J.; Higashi, R.; Kopka, J.; Lane, A. N.; Lindon, J. C.; Marriott, P.; Nicholls, A. W.; Reily, M. D.; Thaden, J. J.; Viant, M. R., Proposed minimum reporting standards for chemical analysis Chemical Analysis Working Group (CAWG) Metabolomics Standards Initiative (MSI). *Metabolomics : Official journal of the Metabolomic Society* **2007**, *3* (3), 211-221.
29. Brown, M.; Dunn, W. B.; Dobson, P.; Patel, Y.; Winder, C. L.; Francis-McIntyre, S.; Begley, P.; Carroll, K.; Broadhurst, D.; Tseng, A.; Swainston, N.; Spasic, I.; Goodacre, R.; Kell, D. B., Mass spectrometry tools and metabolite-specific databases for molecular identification in metabolomics. *The Analyst* **2009**, *134* (7), 1322-32.
30. Horowitz, J. D.; Sia, S. T.; Macdonald, P. S.; Goble, A. J.; Louis, W. J., Perhexiline maleate treatment for severe angina pectoris--correlations with pharmacokinetics. *International journal of cardiology* **1986**, *13* (2), 219-29.
31. Dimitrow, P. P.; Undas, A.; Wolkow, P.; Tracz, W.; Dubiel, J. S., Enhanced oxidative stress in hypertrophic cardiomyopathy. *Pharmacological reports : PR* **2009**, *61* (3), 491-5;
32. Nakamura, K.; Kusano, K. F.; Matsubara, H.; Nakamura, Y.; Miura, A.; Nishii, N.; Banba, K.; Nagase, S.; Miyaji, K.; Morita, H.; Saito, H.; Emori, T.; Ohe, T., Relationship between oxidative stress and systolic dysfunction in patients with hypertrophic cardiomyopathy. *Journal of cardiac failure* **2005**, *11* (2), 117-23.
33. Côté, F.; Fligny, C.; Fromes, Y.; Mallet, J.; Vodjdani, G., Recent advances in understanding serotonin regulation of cardiovascular function. *Trends in molecular medicine* **2004**, *10*(5), 232-8.
34. Fligny, C.; Fromes, Y.; Bonnin, P.; Darmon, M.; Bayard, E.; Launay, J. M.; Cote, F.; Mallet, J.; Vodjdani, G., Maternal serotonin influences cardiac function in adult offspring. *FASEB journal : official publication of the Federation of American Societies for Experimental Biology* **2008**, *22* (7), 2340-9.
35. Reid, J. V., Trial of tryptophan prophylaxis in patients liable to African cardiomyopathy. *South African medical journal = Suid-Afrikaanse tydskrif vir geneeskunde* **1970**, *44* (25), 732-5.

36. Sole, M. J.; Shum, A.; Van Loon, G. R., Serotonin metabolism in the normal and failing hamster heart. *Circulation research* **1979**, *45* (5), 629-34.

Figure 1.

Echocardiography of perhexiline- and placebo-treated *Mybpc3* KI mice. For technical reasons, only 5 perhexiline-treated *Mybpc3* KI mice could be assessed. LV end-diastolic anterior wall thickness and calculated LV mass show a statistically significant change between placebo and perhexiline treated animals (* $p < 0.05$, ** $p < 0.01$). LV fractional shortening (FS) did not show a statistically significant change. Morphometric parameters bodyweight (BW) and whole heart weight (HW) to BW ratio were not significantly altered by the perhexiline-treatment; for full set of morphometric data see Table SI-1.

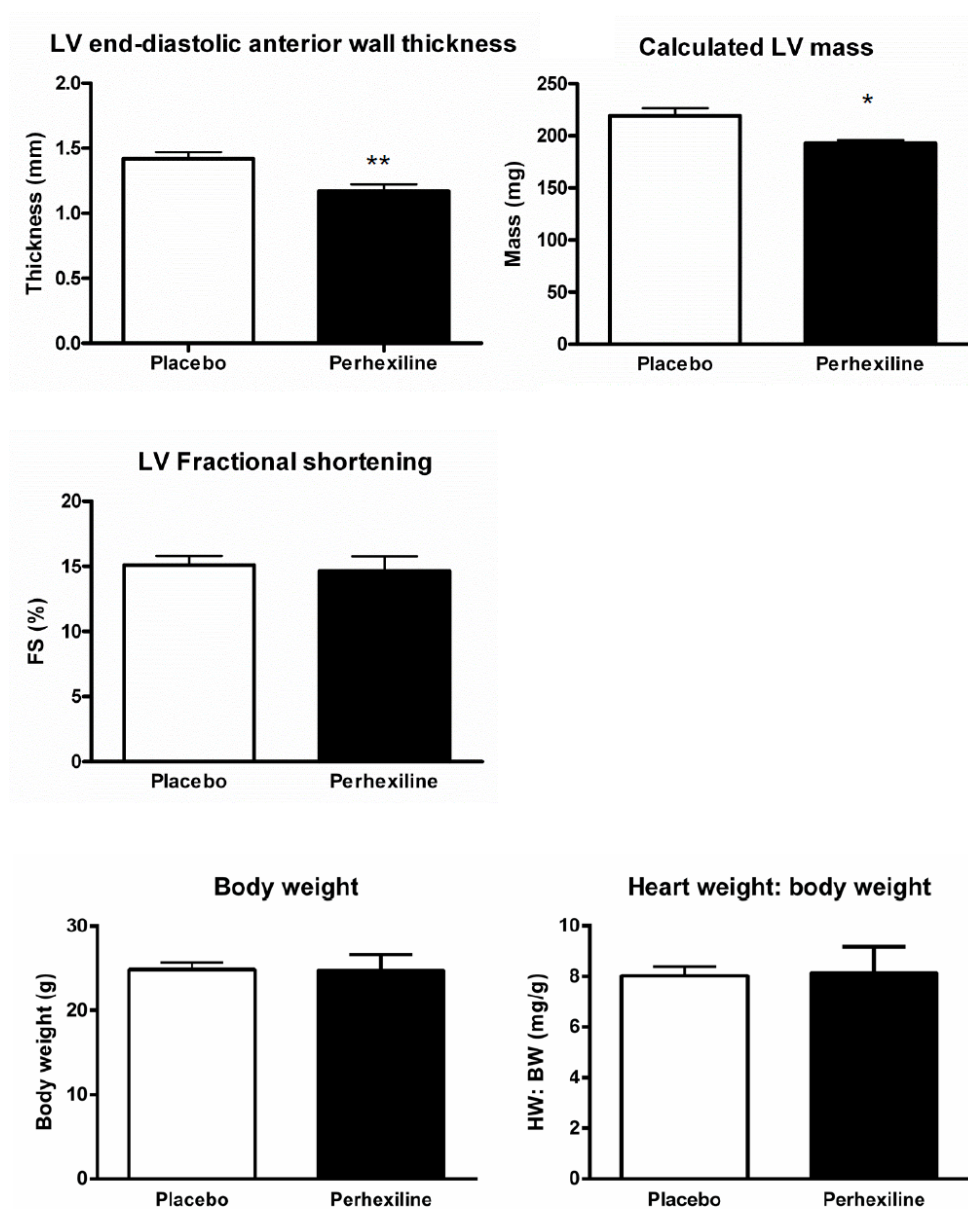


Figure 2.

Principal components analysis scores plot for positive ion mode data. PC1 vs. PC3 is shown and indicate separation of placebo-treated (red triangles) and perhexiline-treated (black circle) animals.

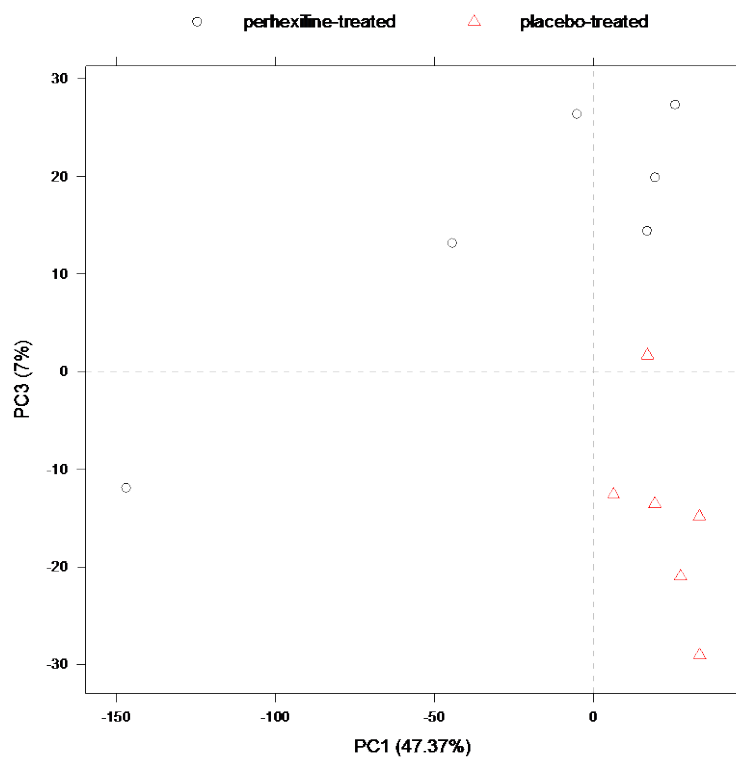


Table 1.

Summary of metabolites highlighted as biologically important. Metabolites are grouped in to classes based on metabolic function or structural similarity. Results for Wilcoxon–Mann–Whitney test are shown with the relative fold-change (median placebo-treated/median perhexiline-treated) and associated 95% confidence limits. Where one metabolite feature can be annotated as multiple metabolites, each metabolite is separated by AND/OR. All metabolite annotations are reported at level 2 (putatively annotated compounds) according to MSI reporting standards²⁸

Metabolite	Fold change (placebo-treated /perhexiline-treated)	P-value
ACYL CARNITINES		
Butanoylcarnitine	0.34 (0.18,1.97)	0.0163
Tetradecenoylcarnitine	0.63 (0.43,1.08)	0.0285
Hexanoylcarnitine	0.74 (0.59,0.97)	0.0209
Decanoylcarnitine	0.75 (0.58,0.99)	0.0283
2-Methylbutyrylcarnitine and/or Isovalerylcarnitine	1.32 (1.08,1.59)	0.0163
Tetradecanoylcarnitine	1.37 (1.11,1.74)	0.0330
Octanoylcarnitine	1.52 (1.05,2.42)	0.0472
Acetylcarnitine	1.71 (1.12,2.52)	0.0163
AMINO ACIDS AND RELATED METABOLITES		
Tyrosine	0.55 (0.30,1.80)	0.0143
Tryptophan	0.75 (0.63,0.91)	0.0090
Indoleamine	1.22 (1.06,1.42)	0.0090
Hydroxykynurenine	1.35 (1.06,1.82)	0.0163
N-Acetyl-tryptophan	1.42 (1.09,1.95)	0.0330

FATTY ACIDS AND RELATED METABOLITES		
nonenoic acid	0.29 (0.12,0.63)	0.0090
hydroxy-tetradecadienoate	0.30 (0.09,0.63)	0.0143
Hydroxy-oxo-heptanedioate	0.49 (0.29,1.61)	0.0106
hydroxyoctanoic acid	0.50 (0.39,0.63)	0.0090
Dodecenedioic acid AND/OR dioxo-dodecanoic acid	0.51 (0.33,0.75)	0.0176
hexadecenoic acid	0.51 (0.30,0.76)	0.0163
dioxo-decanoic acid AND/OR Decenedioic acid	0.58 (0.35,1.61)	0.0163
Dihydroxyoctadecanoic acid AND/OR methyl-hexadecanoic acid	0.59 (0.37,1.36)	0.0250
Epoxyoctadecanoic acid AND/OR Hydroxyoctadecenoic acid AND/OR oxo-octadecanoic acid	0.59 (0.34,2.26)	0.0176
Hydroxystearate	0.65 (0.48,0.94)	0.0176
Hydroxyhexanoic acid	0.68 (0.56,0.86)	0.0090
10-Hydroxydecanoic acid	0.71 (0.58,0.88)	0.0090
oxo-decatetraenoic acid AND/OR Hexanoic acid	0.71 (0.60,0.86)	0.0090
hydroxy-dodecenoic acid AND/OR oxo-dodecanoic acid	0.75 (0.63,0.89)	0.0104
Icosatetraenoic acid AND/OR eicosatetraenoic acid	0.75 (0.61,0.93)	0.0283
Decatetraenedioic acid	0.78 (0.65,0.97)	0.0090
octadecadienoic acid	1.22 (1.06,1.43)	0.0163
hydroxy-hexadecanoic acid	1.24 (1.02,1.55)	0.0163
oxo-docosanoic acid	1.25 (0.95,1.70)	0.0472
Tetracosatetraenoic acid	1.27 (1.02,1.54)	0.0283

Octadecatrienoic acid	1.28 (1.08,1.52)	0.0163
Dodecatetraenedioic acid	1.32 (1.05,1.70)	0.0250
Icosatetraenoic acid AND/OR eicosatetraenoic acid	1.35 (1.09,1.62)	0.0209
Heneicosanedioic acid	1.37 (1.01,2.01)	0.0446
Octadecenoic acid	2.24 (1.36,3.70)	0.0163
GLUTATHIONE AND RELATED METABOLITES		
Reduced glutathione	0.76 (0.62,0.93)	0.0250
GLYCEROL AND RELATED METABOLISM		
Glycerophosphocholine	0.65 (0.42,1.47)	0.0163
Glycerol-phosphate	1.27 (1.12,1.44)	0.0090
Glycerol	1.51 (1.17,1.91)	0.0039
OTHER METABOLITES		
Choline	0.63 (0.45,0.83)	0.0105
Taurine	0.70 (0.62,0.79)	0.0062
Creatinine	0.72 (0.61,0.88)	0.0090
PANTETHEINE METABOLISM		
Pantoate	0.21 (0.07,0.48)	0.0090
S-Acetylphosphopantetheine	0.42 (0.26,0.96)	0.0433
Pantothenic acid	0.69 (0.57,0.86)	0.0163

D-4'-Phosphopantothenate	0.76 (0.61,0.97)	0.0176
Pantetheine 4'-phosphate	0.78 (0.60,0.99)	0.0283
Pantetheine	1.45 (1.19,1.72)	0.0163
SUGARS AND RELATED METABOLITES		
Ribose phosphate AND/OR Xylose phosphate AND/OR Arabinose phosphate AND/OR Xylulose phosphate	0.45 (0.25,2.19)	0.0105
Hexose phosphate (e.g. glucose phosphate OR fructose phosphate)	0.79 (0.70,0.91)	0.0163
Glycerate biphosphate	1.33 (1.07,1.70)	0.0250
Glyceraldehyde 3-phosphate AND/OR Dihydroxyacetone phosphate	1.34 (1.05,1.82)	0.0163
Hexose sugar (e.g. glucose or fructose)	1.42 (1.18,1.69)	0.0104
TCA CYCLE		
Malate	0.69 (0.54,0.94)	0.0062
Citrate AND/OR Isocitrate	0.75 (0.65,0.86)	0.0090
Succinate	1.33 (1.09,1.70)	0.0039
Fumarate AND/OR Maleic acid	1.43 (1.14,1.79)	0.0039